J. of Supercritical Fluids 88 (2014) 46–55

Contents lists available at ScienceDirect

The Journal of Supercritical Fluids

journal homepage: www.elsevier.com/locate/supflu

High pressure density and solubility for the CO_2 + 1-ethyl-3-methylimidazolium ethylsulfate system

Pedro J. Carvalho[a], Teresa Regueira[b], Josefa Fernández[b], Luis Lugo[b,c], Javid Safarov[d], Egon Hassel[d], João A.P. Coutinho[a,*]

[a] Departamento de Química, CICECO, Universidade de Aveiro, 3810-193 Aveiro, Portugal
[b] Laboratorio de Propiedades Termofísicas, Departamento de Física Aplicada, Universidade de Santiago de Compostela, E1782 Santiago de Compostela, Spain
[c] Departamento de Física Aplicada, Facultade de Ciencias, Universidade de Vigo, 36310 Vigo, Spain
[d] Institute of Technical Thermodynamics, University of Rostock, Albert-Einstein-Str. 2, D-18059 Rostock, Germany

ARTICLE INFO

Article history:
Received 7 January 2014
Received in revised form 24 January 2014
Accepted 25 January 2014

Keywords:
Ionic liquids
Carbon dioxide
Solubility
Density
High pressure
ILs

ABSTRACT

The solubility and density of the CO_2 + 1-ethyl-3-methylimidazolium ethylsulfate system were investigated. The carbon dioxide solubility in the IL was measured in the temperature range 273–413 K, for pressure up to 5 MPa and CO_2 mole fractions ranging from 0.02 to 0.5 using the isochoric method, while the system density was carried out at temperatures ranging from 278.15 K to 398.15 K, pressures from 10 MPa to 120 MPa and 0.2, 0.4, 0.7 and 0.8 CO_2 mole fractions. Similar to what was previously observed for phosphonate-based ILs, the ionic liquid high polarity leads to positive deviations from ideality resulting from unfavorable interactions with the CO_2.

The results from the density and solubility derived properties show that the system presents important negative excess molar volumes, over the whole range of compositions and temperatures, and a negative entropy of solvation that suggests an increase in ordering of the solvent molecules surrounding the solute. The observed negative excess molar volumes result from the large difference between the molecular volumes of the species involved, with the small carbon dioxide molecules occupying the empty spaces between the larger IL ions, supporting the notion that the carbon dioxide, upon dissolution, occupies essentially the bulk free volume since the IL does not significantly expand upon gas absorption. These results portray ionic liquids as a porous media, like a soft sponge, with a huge free volume in which large amounts of carbon dioxide are able to accommodate during the dissolution process.

1. Introduction

Outstanding properties, allied to the possibility of fine-tuning them to target a specific application or overcome current process and/or legal limitations, have made ionic liquids (ILs) one of the most interesting, relevant and, consequently, studied solvents of the decade.

The replacement of volatile organic compounds on gas separation processes rose as one of the most promising applications for ILs, with a great deal of work being carried on solubilities and thermophysical properties of ILs + carbon dioxide (CO_2) binary systems. Despite the large amount of work reported in literature, the mechanism of solvation is still not widely accepted. Several authors have complemented experimental measurements of thermophysical and thermodynamic properties with spectroscopy measurements [1–8] to ultimately understand the mechanism of solvation and the interactions that control the CO_2 solubility in ILs. Even though the interactions observed by spectroscopic techniques are of high relevance for an understanding of the solvation of CO_2, they are not enough to fully explain its solubility or the deviations to the ideal behavior observed on these systems [9–11]. In fact, based on the solubility and spectroscopic evidence for the interactions of CO_2 with BF_4 and PF_6 anions, Kazarian et al. [12] were the first to recognize that "*the strength of the interactions cannot be solely responsible for the solubility of* CO_2 *in ionic liquids*". Later, Seki et al. [8] reported that, although the interactions of CO_2 with BF_4 and PF_6 anion-based ILs are stronger than those with the NTf_2, the solubility of CO_2 on these ILs is larger than in the former, and thus the interactions alone are not enough to provide an explanation for the CO_2 sorption. Furthermore, these authors recognize that the strong Lewis acid–base interactions observed have no promotional effect on the solubility of CO_2 [8]. Shi and Maginn [13] have shown, through atomistic simulation, that the $[C_6mim][NTf_2]$ underlying structure is not disturbed upon the CO_2 dissolution. Moreover, the authors have shown that the CO_2 absorbs mainly in regions of free volume and that CO_2 associates strongly with the ions, "collapsing" the liquid and reducing the overall volume expansion. Since the IL does not present cavities

* Corresponding author.
E-mail address: jcoutinho@ua.pt (J.A.P. Coutinho).

0896-8446/$ – see front matter © 2014 Elsevier B.V. All rights reserved.
http://dx.doi.org/10.1016/j.supflu.2014.01.011

large enough to accommodate the CO_2 [14] the authors stated that the cations and anions slightly adjust their relative positions so that CO_2 can "*just fit in*" [13]. Recently we have shown [15], through Raman spectroscopy, that CO_2 absorbs in the existing voids of the [C_4mim][TFA] ion pairs. Furthermore, the results show that the IL is able to accommodate large amounts of CO_2 without having its short-range local structure significantly perturbed [15].

Looking at understanding the high CO_2 sorption in a series of imidazolium-based ionic liquids Aki et al. [16] evaluated the IL + CO_2 molar volumes and volume expansions, showing that the ILs volume expansions appear to be independent of the choice of the IL and present considerable lower volume expansions than those of common organic solvents. Moreover, the authors stated that since the ILs volume does not change significantly upon dissolution of large amounts of CO_2, the solvent strength of these mixtures should decrease marginally when CO_2 is added [16].

In a previously publication [9] the non-ideality of CO_2 in ILs and other low volatile solvents, with which CO_2 is known to form electron donor–acceptor (EDA) complexes, was investigated. It was shown that the deviations from the ideality observed were not related with the stability of the EDA complex formed and, in most cases, the deviations were small and dominated by entropic effects. Furthermore, we have shown that if expressed in a molality scale, the pressure versus concentration phase diagrams of CO_2 in nonvolatile solvents are, within the uncertainty of the experimental data, solvent independent. Later we were able to relate the observed non-ideality of these systems with the polarity of the ionic liquid [10].

Aiming at further exploring the mechanism behind the absorption of carbon dioxide in ionic liquids the present work investigates the volume expansion, liquid phase non-ideality, enthalpies and entropies of solvation through the measurement of solubility and density of an highly polar IL + CO_2 binary mixture. It will be shown here that, in agreement to what few other authors [16,17] have reported, the IL does not expand upon the gas addition and that the carbon dioxide, upon dissolution, occupies only the bulk free volume. These findings are further supported by the enthalpies of solvation and entropy of solvation derived from solubility data.

2. Experimental

2.1. Chemicals

The 1-ethyl-3-methylimidazolium ethylsulfate, [C_2mim][$EtSO_4$], was acquired from Io-Li-Tec, with mass fraction purities higher than 99%. Prior to the measurements, all the ionic liquids were dried under moderate vacuum (1 Pa) at room temperatures for at least 48 h to assure that water and volatile compounds were removed and consequently the influence of these impurities on the measurements minimized. The water concentration of dried IL was determined through Karl Fischer titration and was less than 3×10^{-4} mass fraction.

The carbon dioxide, CO_2, with a mass fraction purity of 0.99998 was purchased from Air Liquide and Westfalen AG, Germany, for the density and vapor–liquid equilibria measurements, respectively. The CO_2 was used without further purification.

2.2. Solubility measurements

The experimental setup consists of three main parts: (i) gas reservoir, (ii) stainless steel equilibrium cell and (iii) electronic tracking system. The gas reservoir structure is made of two 19 mm parallel expanded plastic slab materials (Kömacel, Germany), with vacuum in between them. This structure confers low heat exchange and high insulation against temperature perturbations. Three high pressure gas tanks (two with 150 cm^3 and one with 300 cm^3) are kept thermostated, inside the gas reservoir, by means of a eight parallel hot foils (Conrad Electronic SE, Germany) placed in the back side of an aluminum heating plate and able to control the temperature within 50 mK. The temperature is measured by means of a 1/10 DIN Class B Pt100 probe (Temperatur Messelemente Hettstedt GmbH, Germany) with an uncertainty of 0.02 K. The gas pressure, in the gas reservoir, is measured by means of pressure transducer (PAA33X-V-100, Omega Engineering) able to operate from 0 MPa to 10 MPa with an uncertainty of 0.1%. For measurements close to the CO_2 critical temperature (304.1282 K), the gas reservoir temperature was set to a constant value (303.15 K).

The equilibrium cell, made of stainless steel and with a volume of 139.96 cm^3, is placed inside a metal reservoir and connected to the gas reservoir through a high pressure valve. Silicone oil (Korasilon Öl M 20, Kurt Obermeier GmbH & Co. KG, Germany) circulates through the metal reservoir and around the equilibrium cell by means of a circulator bath (Kälte-Umwälzthermostat LAUDA ECO RE 415 Gold, Germany), directly managed to the metal reservoir and able to control the temperature within 0.02 K.

Due to the well-known high CO_2 solubility in ILs, a large gas reservoir (619.57 cm^3), apart from the measuring cell volume, was used. The setup volumes were previously calibrated using several ideal gases, like Ar, He and H_2. A detailed description of the setup can be found in a previous work [18].

Before each measurement, the measuring cell was washed with water and acetone and vacuum was applied for 4–5 h to ensure the complete removal of any volatile compound. A fixed amount of IL was introduced inside the measuring cell by weighting the filling flask before and after the filling procedure using a high precision balance with an accuracy of 1 mg (Sartorius ED224S, Germany). Vacuum was then applied again for 4–5 h in order to assure no interference from atmospheric gases adsorbed during the manipulation.

With the setup under vacuum, the valve connecting the gas reservoir and the equilibrium cell is closed. The valve of the external CO_2 tank is opened and the carbon dioxide allowed to fill the gas reservoir and the gas line. The setup temperature (gas reservoir and equilibrium cell) is allowed to stabilize and the CO_2 target pressure set, by regulating it through a pressure reducer (AirCom Pneumatic GmbH, Germany). The stabilization of the CO_2 pressure and temperature takes approximately 3–5 h. Once stabilized, the mass of the gas in the gas reservoir is determined knowing the volume, temperature, pressure and CO_2 density:

$$m_{CO_2} = \rho_{CO_2} V \quad (1)$$

where V is the volume of the gas reservoir. The valve connecting the gas reservoir and the equilibrium cell is then open and the solubility of CO_2 in the IL is followed by monitoring the decrease of the system pressure. The stabilization of the experimental pressure indicates the end of the solution process and gives the total amount of CO_2 in the IL, for every temperature studied. The volume increase ΔV of the IL in the measuring cell, as the result of carbon dioxide solubility, is very small and can be neglected. Experiments were carried out in four different pressure steps.

2.3. Density measurements

The experimental setup consists of a fully automated computer-operated technique based on a vibrating tube densimeter (Anton Paar HPM) able to operate up to 120 MPa and in the temperature range 278.15–398.15 K [19]. The densimeter consists of two different units: the measurement cell (DMA HPM) and the electronic processing unit (mPDS 2000V3). The uncertainty of vibrating

period, τ, data is 1 ns for periods around 2.7 ms. The temperature is controlled through a thermostatic bath (Polyscience 9102) directly managed to inlet/outlet ports, that regulate the temperature within an uncertainty of 0.01 K. The temperature is measured by means of a Pt100 probe, previously calibrated and with an uncertainty of 0.02 K, located inside the cell.

A loading technique for systems containing two components that are in different states, liquid and gas, at atmospheric pressure and ambient temperature was used according to the procedure previously proposed [20]. This loading procedure has proven to assure an accurate density measurement by a proper mixture manipulation and transfer. The loading system consists of two syringe ISCO Teledyne pumps (model 260D) coupled with electronic valves that dispenses the compounds through stainless-steel tubes at programmable constant flow rates. These pumps, with a capacity of 266 cm^3, are thermostated and filled under pressure allowing thus, to work with supercritical fluids at pressures up to 52 MPa. A schematic of the experimental setup can be seen elsewhere [20]. Moreover, a pressure limiting valve (Grove Mity Mite model S-91XW), placed at the end of the pressure line, allows the mixture to be transferred to the densimeter through an isobaric process. The composition of the mixtures is determined through the ISCO pumps flow rates.

The pressure is automatically generated by means of a step by step engine (ACP&D limited type 6530-24 with a gearbox) connected to a compressor (HiP 50-5.75-30) and is measured by means of a pressure transducer (HBM Digibar II K-PE300), previously calibrated and able to follow the system pressure up to 200 MPa with an uncertainty of 0.02 MPa. Both the temperature probe and the pressure transducer are connected to an Agilent 34970A data acquisition unit that allows the operator to follow both signals in real time. Except for the filling and cleaning operations the experimental procedure is fully automated. A detailed description and a schematic figure of the experimental setup can be found elsewhere [20].

The densimeter was calibrated following the procedure proposed by Lagourette et al. [21] and later modified by Comuñas et al. [22]. Milli-Q water was employed as reference fluid at temperatures between 278.15 K and 348.15 K and pressures between 0.1 MPa and 120 MPa and also at T = 373.15 K and T = 398.15 K for pressures higher than 0.1 MPa, whereas *n*-decane was used as reference fluid at T = 373.15 K and T = 398.15 K and at 0.1 MPa. The expanded (k = 2) uncertainty of the density with this technique was rigorously calculated by Segovia et al. [23] and found to be 0.7×10^{-3} g cm^{-3} for temperatures below 373.15 K, 5×10^{-3} g cm^{-3} at 373.15 K and 398.15 K and p = 0.1 MPa, and 3×10^{-3} g cm^{-3} in other cases, i.e. at $T \geq$ 373.15 K and p > 0.1 MPa.

3. Results and discussion

3.1. Solubility measurements

The CO_2 solubility in [C_2mim][$EtSO_4$] was investigated in the temperature range 273–413 K, for pressure up to 5 MPa and CO_2 mole fractions ranging from 0.02 to 0.5 using the isochoric method. This method has been found suitable for gas solubility in ILs, since the ILs negligible vapor pressure ensures that the gas phase remains pure gas and therefore, changes on pressure are due to gas sorption. The experimental solubility data is reported in Table 1 and depicted in Fig. 1. In Table 2, pressure dependency of interpolated CO_2 solubility in [C_2mim][$EtSO_4$] is presented in molality and mole fraction of solute at selected temperatures. The solubility follows the typical solubility behavior decreasing with temperature and increasing with pressure as commonly observed for other CO_2-ILs binary systems [11,18,24–27].

Table 1
Bubble point data and fugacity coefficients of pure CO_2, $\varphi_{CO_2}(T, p)$, of the binary system CO_2 + [C_2mim][$EtSO_4$].

T (K)	p (MPa)	m_{CO_2} (mol kg^{-1})	x_{CO_2} (mole fraction)	$\varphi_{CO_2}(T, p)$
273.15	0.372	0.3972	0.071	0.975447
273.15	1.110	1.0143	0.193	0.927060
273.15	2.424	2.2790	0.350	0.841261
293.15	0.393	0.2715	0.060	0.979442
293.15	1.152	0.7945	0.158	0.940054
293.15	2.525	1.7237	0.289	0.869589
293.15	4.324	3.2401	0.434	0.777418
313.15	0.407	0.1973	0.045	0.982887
313.15	1.191	0.5844	0.121	0.950212
313.15	2.610	1.2322	0.226	0.891929
313.15	4.472	2.2988	0.352	0.816674
333.15	0.417	0.1509	0.034	0.985747
333.15	1.218	0.4608	0.098	0.958625
333.15	2.668	0.9445	0.183	0.910332
333.15	4.562	1.7937	0.298	0.848656
353.15	0.424	0.1247	0.029	0.988114
353.15	1.238	0.3837	0.083	0.965517
353.15	2.710	0.7683	0.154	0.925370
353.15	4.625	1.4699	0.258	0.874467
373.15	0.429	0.1110	0.026	0.990068
373.15	1.255	0.3220	0.071	0.971135
373.15	2.742	0.6556	0.134	0.937676
373.15	4.672	1.2501	0.228	0.895429
393.15	0.434	0.0954	0.022	0.991656
393.15	1.268	0.2850	0.063	0.975788
393.15	2.769	0.5654	0.118	0.947771
393.15	4.709	1.0898	0.205	0.912587
413.15	0.438	0.0853	0.020	0.992980
413.15	1.279	0.2576	0.057	0.979646
413.15	2.792	0.4933	0.104	0.956128
413.15	4.738	0.9841	0.189	0.926768

Standard uncertainties u are $u(T)$ = ±0.015 K, $u(P)$ = ±0.15%, $u(m_{CO_2})$ = ±0.001 mol kg^{-1} and $u(x_{CO_2})$ = ±0.0005 mole fraction.

The solubility of the binary system CO_2 + [C_2mim][$EtSO_4$] has been reported in the literature before by Blanchard et al. [28] at 313.15, 323.15 and 333.15 K, Jalili et al. [29] at 303.15–353.15 K, recently by Bermejo et al. [30] at 298 and 348 K, Soriano et al. [31] at 303.2–343.2 K, by Supasitmongkol and Styring [32] at 298 K and Petermann et al. [33] a 298.15 K. Blanchard et al. [28], Jalili et al. [29] and Supasitmongkol and Styring [32] used the isochoric method similar to that used here, while Bermejo et al. [30] used a magnetic suspension balance, Soriano et al. [31] used a thermogravimetric microbalance and Petermann et al. [33] a gravimetric–volumetric method. Fig. 2 depicts the literature data plotted against the experimental data obtained here. As can be observed, not only the data available in literature presents considerable discrepancies among the different authors but also important inconsistencies within the same data source. Blanchard et al. [28] reports equilibrium pressures that span across the authors different temperatures; with the 313 K isotherm presenting both lower, for CO_2 mole fractions lower than 0.2, and higher CO_2 solubilities than the 323 K isotherm, for higher CO_2 compositions. Bermejo et al. [30] present, depending on the temperature, either a complete linear equilibrium pressure or a pronounced curvature for the same gas low mole fraction region. Furthermore, for the higher temperature, not only the isotherm presents unusual variations but most important a curvature more pronounced than expected. Overall, the experimental data reported here presents lower equilibrium pressures than those reported by these authors, with an average pressure deviation ($\overline{\Delta p}$) of 0.11, 1.6 and 0.4 MPa, and consequently a percentage average deviation (%AD) of 16%, 29% and 17%, for the Blanchard et al. [28], Jalili et al. [29] and Soriano et al. [31] data, respectively. The data from Supasitmongkol and Styring [32] was not represented since the authors present equilibrium pressures in bar units that are not reasonable, and even if one assumes the

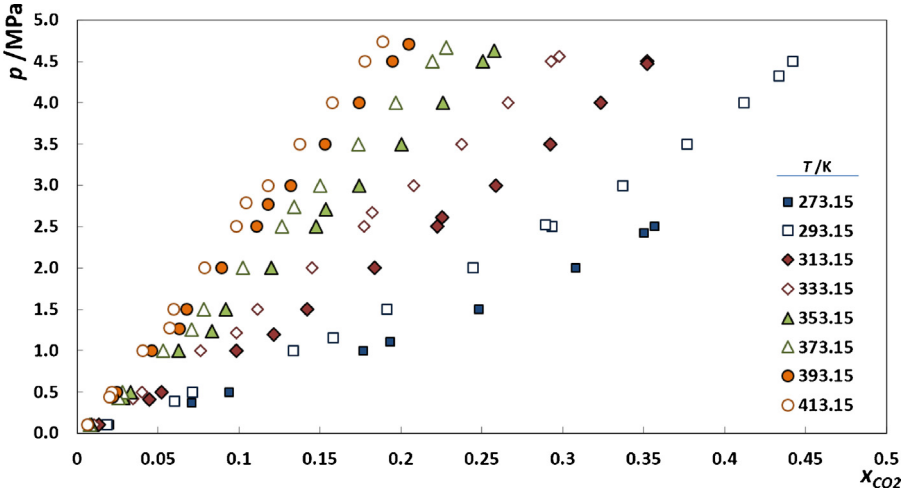

Fig. 1. Pressure–composition phase diagram for the binary system CO_2 + [C_2mim][$EtSO_4$] system.

Table 2
Interpolated bubble point data of the binary system CO_2 + [C_2mim][$EtSO_4$].

P (MPa)	0.101	0.5	1.0	1.5	2.0	2.5	3.0	3.5	4.0	4.5
T (K)	m_{CO_2} (mol kg^{-1})									
413.15	0.0302	0.0927	0.1760	0.2649	0.3595	0.4597	0.5655	0.6769	0.7940	0.9166
393.15	0.0311	0.1054	0.2030	0.3056	0.4133	0.5259	0.6436	0.7663	0.8941	1.0268
373.15	0.0350	0.1222	0.2365	0.3562	0.4815	0.6123	0.7486	0.8904	1.0377	1.1905
353.15	0.0401	0.1446	0.2812	0.4243	0.5737	0.7295	0.8917	1.0602	1.2351	1.4163
333.15	0.0470	0.1778	0.3485	0.5269	0.7129	0.9066	1.1080	1.3170	1.5337	1.7580
313.15	0.0590	0.2350	0.4635	0.7007	0.9467	1.2015	1.4650	1.7374	2.0185	2.3085
293.15	0.0813	0.3312	0.6585	1.0014	1.3600	1.7343	2.1242	2.5298	2.9511	3.3880
273.15	0.1129	0.4743	0.9330	1.3984	1.8703	2.3488				
T (K)	x_{CO_2} mole fraction									
413.15	0.0066	0.0216	0.0405	0.0596	0.0788	0.0982	0.1178	0.1376	0.1575	0.1777
393.15	0.0069	0.0244	0.0462	0.0679	0.0894	0.1108	0.1321	0.1532	0.1741	0.1950
373.15	0.0078	0.0282	0.0534	0.0782	0.1026	0.1267	0.1504	0.1737	0.1967	0.2193
353.15	0.0089	0.0331	0.0628	0.0918	0.1200	0.1476	0.1744	0.2004	0.2258	0.2504
333.15	0.0104	0.0403	0.0765	0.1113	0.1449	0.1772	0.2081	0.2377	0.2661	0.2931
313.15	0.0134	0.0522	0.0985	0.1423	0.1836	0.2224	0.2586	0.2924	0.3235	0.3522
293.15	0.0185	0.0714	0.1337	0.1914	0.2445	0.2932	0.3372	0.3768	0.4118	0.4422
273.15	0.0199	0.0940	0.1767	0.2480	0.3080	0.3567				

Standard uncertainties u are $u(T) = \pm 0.015$ K, $u(P) = \pm 0.1\%$, $u(m_{CO_2}) = \pm 0.001$ mol kg^{-1} and $u(x_{CO_2}) = \pm 0.0005$ mole fraction.

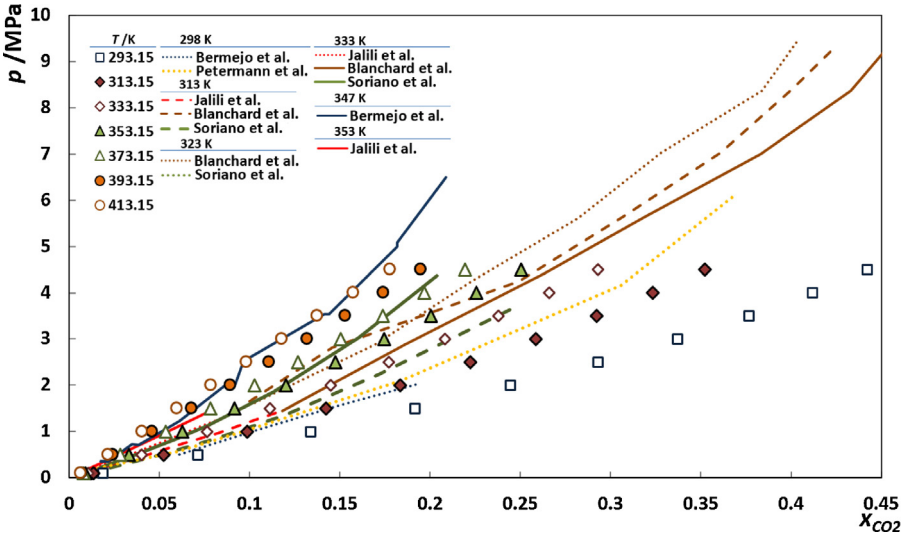

Fig. 2. Pressure–composition phase diagram for the binary system CO_2 + [C_2mim][$EtSO_4$]. Symbols represent the experimental data points and the lines (solid, dots and dashed) represent the data from: brown lines – Blanchard et al. [28], red lines – Jalili et al. [29], blue lines – Bermejo et al. [34], green lines – Soriano et al. [31] and yellow lines – Petermann et al. [33]. (For interpretation of the references to color in this figure legend, the reader is referred to the web version of the article.)

Table 3
The values of calculated Henry constant (k_{H,CO_2}, MPa) resulting from the extrapolations, free energy of solvation $\Delta_{sol}G$, enthalpy of solvation $\Delta_{sol}H$, entropy of solvation $\Delta_{sol}S$ and heat capacity of solvation $\Delta_{sol}C_p$ at various temperatures T.

T (K)	k_{H,CO_2} (MPa)	$\ln(k_{H,CO_2}/p_0)$	$\Delta_{sol}G$ (J mol^{-1})	$\Delta_{sol}H$ (J mol^{-1})	$\Delta_{sol}S$ (J mol^{-1} K)	$\Delta_{sol}C_p$ (J mol^{-1} K)
413.15	23.30	5.4510	18,723.93	−7739.23	−64.05	35.15
393.15	20.40	5.3181	17,383.07	−8474.87	−65.77	37.65
373.15	17.55	5.1676	16,031.92	−9246.22	−67.74	39.68
353.15	14.93	5.0060	14,697.94	−10,051.60	−70.08	41.23
333.15	12.17	4.8016	13,299.40	−10,886.98	−72.60	42.31
313.15	9.25	4.5272	11,786.72	−11,744.48	−75.14	42.92
293.15	6.65	4.1972	10,229.63	−12,610.15	−77.91	43.06
273.15	4.56	3.8199	8674.89	−13,460.14	−81.04	42.72

correct data to be in MPa, assuming thus a mistype, their data at 298 K stands below our 273 K isotherm and, naturally, well below those of Bermejo et al. [34] and Petermann et al. [33] at 298 K. Furthermore, the authors present a Henry's constant for the system of 13.45 bar that, by analyzing the experimental data plotted, seems to stand for the Henry's constant of the system [C_4mim][NTf_2]. If one assumes that the correct experimental data are those reported as being for the binary system CO_2 + [C_4mim][NTf_2] and on MPa units, instead of bar units, then the data becomes mostly coincident to that of Bermejo et al. [34] at 298 K. Although some small discrepancies are expected due to the different techniques used, the higher ones are, most probably, the result of impurities. Specially if one take into consideration that methyl sulfate- and ethyl sulfate-based ILs are not stable in the presence of water and are keen to hydrolyze to methanol or ethanol and hydrogenate anion, as recently shown by Jacquemin et al. [35].

3.2. Henry's constant

The Henry's law relates the amount of a given gas dissolved in a given type and volume of liquid, at a constant temperature, to the fugacity of that gas in equilibrium with that liquid. Henry's law for an ideal solution with a standard-state fugacity based on infinitely dilute solution can be used to correlate the gas solubility. For binary systems with a non-ideal gas phase Henry's law can be described as

$$y_{CO_2}\varphi_{CO_2}(T,p)p = x_{CO_2}k_{H,CO_2}(T) \tag{2}$$

where y_{CO_2} is the gas composition on the vapor phase, φ_{CO_2} is the gas fugacity coefficient and $k_{H,CO_2}(T)$ is the Henry's constant. For solvents with negligible vapor pressure, like the ILs, the vapor phase can be considered pure gas, $y_{CO_2} = 1$. The fugacity coefficients of pure CO_2 were estimated by using the equation of state of Span and Wagner [36] at the experimental temperatures and pressures. The fugacity coefficient can be rewritten as

$$\varphi_{CO_2}(T,p) = \frac{f_{CO_2}(T,p)}{p} \tag{3}$$

Eq. (2) can, thus, be rewritten in terms of the Henry's constant as

$$f_{CO_2}(T,p) = k_{H,CO_2}(T,p)x_{CO_2} \Leftrightarrow k_{H,CO_2}(T,p) = \frac{f_{CO_2}(T,p)}{x_{CO_2}} \tag{4}$$

Henry's constant represents the linear relationship between the carbon dioxide concentration and experimental pressure, and is only rigorously valid in the dilute region limit

$$k_{H,CO_2}(T,p) = \lim\ x_{x_{CO_2}\to 0}\frac{f_{CO_2}}{x_{CO_2}} \tag{5}$$

and can be estimated by fitting Eq. (4) to the experimental data and calculating the limiting slope as the solubility approaches zero. The Henry's constants obtained are given in Table 3 as function of temperature and as would be expected increase with the temperature.

Thermodynamic properties of solution for the binary system studied can be obtained from the correlation of the Henry's constant through the thermodynamic relations:

$$\Delta_{sol}G = RT\ \ln\left(\frac{k_{H,CO_2}(T,p)}{p^0}\right) \tag{6}$$

$$\Delta_{sol}H = R\left(\frac{\partial\ln((k_{H,CO_2}(T,p))/p^0)}{\partial(1/T)}\right) \tag{7}$$

$$\Delta_{sol}S = \frac{(\Delta_{sol}H - \Delta_{sol}G)}{T} \tag{8}$$

$$\Delta_{sol}C_p = \left(\frac{\partial\Delta_{sol}H}{\partial T}\right)_p \tag{9}$$

where $\Delta_{sol}G$, $\Delta_{sol}H$, $\Delta_{sol}S$ and $\Delta_{sol}C_p$ are the Gibbs free energy of solvation, enthalpy of solvation, entropy of solvation and heat capacity of solvation, respectively. The values obtained for eight temperatures between 273.15 K and 413.15 K are reported in Table 3. The values of Gibbs free energy, enthalpy and entropy of solvation increase with increasing temperature whereas, heat capacity of solvation decreases with increasing temperature. The negative enthalpies of solvation indicate an exothermal solvation process. Similarly, the values of the entropy of solvation are also negative which indicate an increase in order of the solvent molecules surrounding the solute.

The measured CO_2 solubility results in IL as a function of temperature and pressure are fitted to the following Virial equation using the mole fraction dependence:

$$x = \sum_{i=0}^{2} p^i \sum_{j=0}^{2} a_{ij}T^j \tag{10}$$

where the equation coefficients are presented in Table 4.

3.3. Liquid phase non-ideality

In a previous work we have studied the mechanism behind the sorption of carbon dioxide, methane and nitrogen in phosphonate-based ILs, by analysing their deviations from ideality in the liquid phase [11]. Aiming at enhancing the CO_2/CH_4 and CO_2/N_2 selectivities by tunning the IL polarity, it was found that phosphonate-based

Table 4
Eq. (10) a_{ij} coefficients values.

a_{00}	0.04326438342	a_{12}	$0.8367725339 \times 10^{-5}$
a_{01}	$-0.2188628896 \times 10^{-3}$	a_{20}	−0.1636883834
a_{02}	$0.2933127867 \times 10^{-6}$	a_{21}	$0.8445573473 \times 10^{-3}$
a_{10}	1.388163670	a_{22}	$-0.1087556815 \times 10^{-5}$
a_{11}	$-0.6716642754 \times 10^{-2}$		

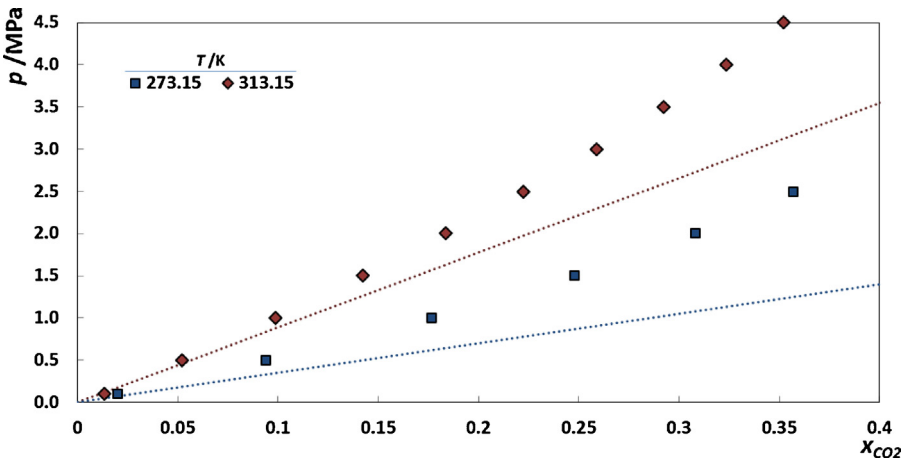

Fig. 3. Pressure–composition phase diagram for the binary system CO_2 + [C_2mim][$EtSO_4$] system. The dashed lines represent the Raoult's law for CO_2 at 273.15 and 313.15 K.

ILs present positive deviations to ideality and therefore lower CO_2 solubilities. Here, the studied sulfate IL presents also positive deviations from ideality, as depicted in Fig. 3. As observed for the phosphonate-based ILs the highly polar sulfate IL presents unfavorable interactions with the CO_2. As previously shown in [9–11], if one targets a highly selective solvent for carbon dioxide separation a delicate balance between the solvent polarity and the molar volume must be established.

3.4. Density measurements

Density measurements for the CO_2 + [C_2mim][$EtSO_4$] system were carried out at temperatures ranging from 278.15 K to 398.15 K, pressures from 10 MPa to 120 MPa and for 0.2, 0.4, 0.7 and 0.8 CO_2 mole fractions. The experimental pressure–volume–temperature (pVT) data obtained are depicted in Fig. 4 and reported in Table 5 along with those previously reported by us [19] for the pure IL and those reported in NIST [37] for pure carbon dioxide. As commonly observed the density increases with the pressure and decreases with the temperature. Furthermore, until a carbon dioxide mole fraction composition of 0.6 the pressure does not have a significant influence on the density. For higher CO_2 mole fractions the densities are greatly affected by the pressure, possibly due to the presence of a liquid–liquid-like region.

The excess volumes were calculated from the measurements according to the following equation and depicted in Fig. 5.

$$\Delta V_m = \left(\frac{x_{IL}M_{IL} + x_{CO_2}M_{CO_2}}{\rho_{mix}}\right) - \left(\frac{x_{IL}M_{IL}}{\rho_{IL}} + \frac{x_{CO_2}M_{CO_2}}{\rho_{CO_2}}\right) \quad (11)$$

where ρ is the density, M the molecular weight and x the molar fraction of the mixture, CO_2 and [C_2mim][$EtSO_4$].

The excess thermodynamic properties, which depend on the composition, temperature, or both, are of great importance in understanding the nature of the molecular interactions present in the binary mixtures. The excess molar volumes are negative over the whole range of compositions and temperatures, as depicted in Fig. 5, and several opposing effects are involved in the mixing process. Similarly to what is observed to other binary systems of CO_2 + molecular liquids, like decane and complex esters [20,38,39], the excess molar volumes become more negative with the temperature increase and pressure decrease. No specific interactions are formed or expected upon the gas sorption but by increasing the dipolar distance the Coulombic interactions are to some extent reduced, promoting thus positive effects, in a small scale, when compared to the negative effects observed. By other hand, the strong negative excess volumes observed for these systems support the physical sorption mechanism of CO_2 in ILs previously proposed [9–11,13,15], with the observed system contraction resulting from the large difference between the molecular volumes and, thus, the small carbon dioxide molecules occupying the empty spaces between the larger volumes of the IL constituents.

3.5. Volume expansion

The volume expansion of the liquid phase of a CO_2-expanded organic solvent is defined as

$$\frac{\Delta V}{V} = \frac{V_{mix}(T, p, x_{CO_2}) - V_{IL}(T, p_0)}{V_{IL}(T, p_0)} \quad (12)$$

where $V_{IL}(T, p_0)$ is the total volume of the pure IL at a specific temperature and reference pressure (0.1 MPa), $V_{mix}(T, p, x_{CO_2})$ represents the total volume of a CO_2-expanded organic solvent with the CO_2 mole fraction of x_{CO_2}. Mathematically, Eq. (12) can be rewritten as

$$\frac{\Delta V}{V} = \frac{1}{1 - x_{CO_2}} \frac{v_{mix}(T, p, x_{CO_2})}{v_{IL}(T, p_0)} - 1 \quad (13)$$

where $V_{IL}(T, p_0)$ and $V_{mix}(T, p, x_{CO_2})$ are the molar volume of the pure organic solvent (IL) and the liquid-phase molar volume, respectively. Eqs. (12) and (13) can be rewritten in terms of the liquid-phase density of the binary mixture, $\rho_{mix}(T, p, x_{CO_2})$, and that of the pure organic solvent, $\rho_{IL}(T, p_0)$:

$$\frac{\Delta V}{V} = \frac{\rho_{IL}(T, p_0)}{\rho_{mix}(T, p, x_{CO_2})} \left(\frac{x_{CO_2}}{1 - x_{CO_2}} \frac{M_{CO_2}}{M_{IL}} + 1\right) - 1 \quad (14)$$

where M_{CO_2} and M_{IL} are the molecular weights of the CO_2 and IL, respectively.

As depicted in Fig. 6 different trends can be clearly identified and tagged to specific families of compounds; with the selected organic solvents presenting large volume expansions and both the studied IL and the alkanes presenting considerably lower volume expansions. The experimental data was taken from literature [40–45]. Volume expansions for the organic solvents, depicted in Fig. 6, have already been discussed by de la Fuente Badilla et al. [46] and Su [47]. The authors have reported volume expansions weakly dependent on the choice of the organic solvent and with large percent expansion, which are in concordance to the compounds high CO_2 chemisorption, depicted in Fig. 6.

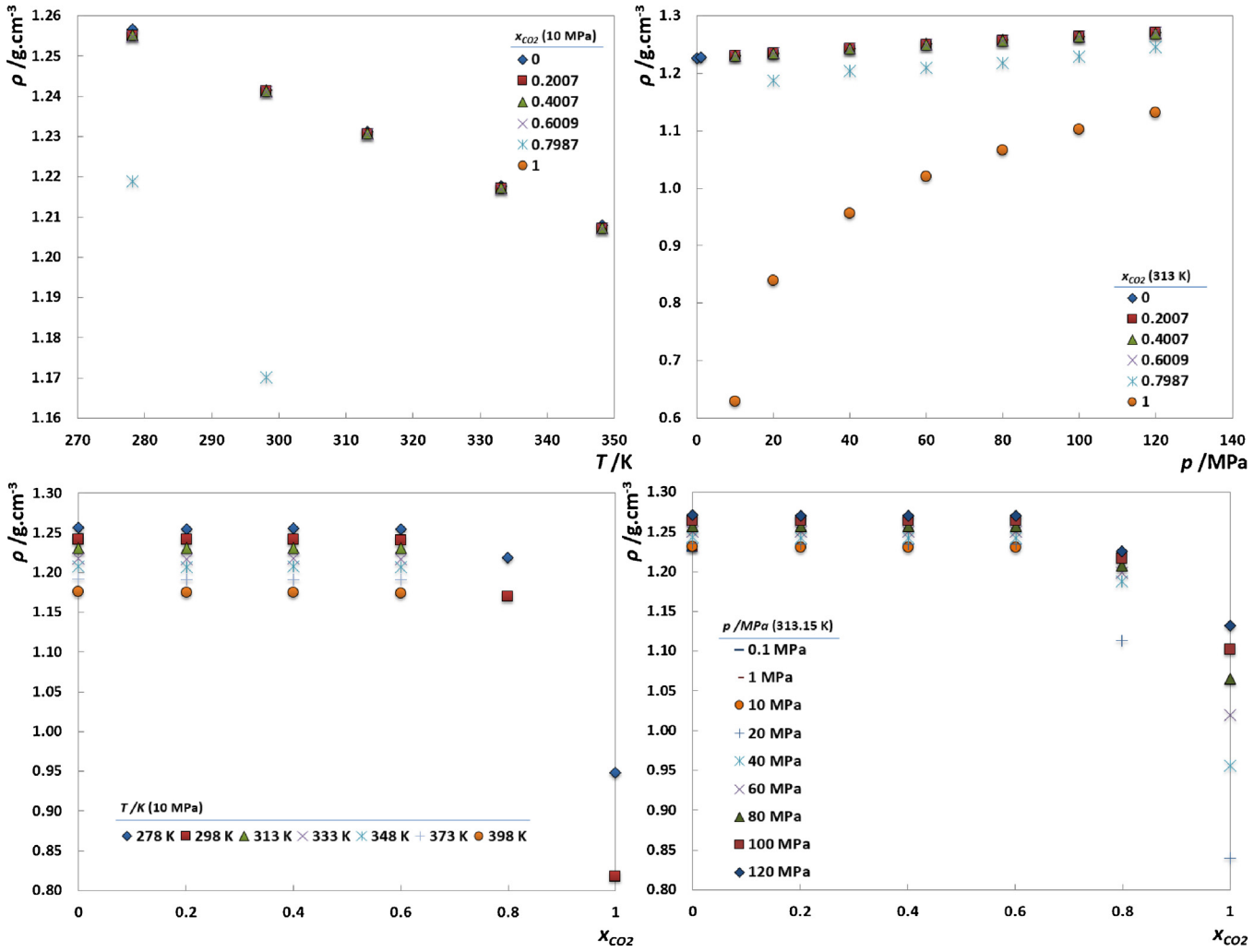

Fig. 4. Density as function of temperature, at 10 MPa (top left), density as function of pressure, at 313.15 K (top right) and density as function of CO_2 composition, at 10 MPa (bottom left) and 313.15 K (bottom right), for the CO_2 + [C_2mim][$EtSO_4$] system. The density of pure CO_2 was taken from NIST [37].

Volume expansions of CO_2-ILs binary systems have also been investigated before by Aki et al. [16]. The authors investigated a series of imidazolium-based ionic liquids and reported similar results, with the ILs volume expansions collapsing into a single curve, at all the temperatures evaluated, and with considerable lower volume expansions than most common organic solvents. In fact the authors stated that the volume expansion appears to be independent of the choice of the IL, even though the molecular weights of the ILs evaluated differ by a factor of 2. Although the ILs low volume expansion stands by itself as an outstanding result, the fact of being independent of the choice of the IL comes, by contrast, counterintuitively, specially if one considers that the CO_2 absorption in common ILs is something else than purely physical [9,10,48]. If a physical absorption mechanism is adopted, with all the carbon dioxide absorbed into the IL free volume then the results becomes understandable.

Another striking result is the similarity of the volume expansion of the ILs and alkanes being very low in both families of compounds. Nonetheless, since both families present physical carbon dioxide absorption and similar solubilities [9], when expressed in molality scale, both the ILs and the alkanes volume expansion corroborate that the carbon dioxide, upon dissolution, occupies only the bulk free volume and that both compound families do not expand upon the gas addition.

de La Fuente Badilla et al. [46] argued that since in the gas-antisolvent process the precipitation of a solute is a consequence of the liquid-phase volume expansion, the relative volume expansion as defined by Eq. (14) is not able to distinguish different solvents in their liquid-phase expansivity and therefore, not suitable to develop criteria for optimum process conditions for the gas-antisolvent process. Thus, the authors identified the Kordikowski et al. [40] equation, based in the molar volumes instead of the total volumes, as the most suitable definition for the relative volume expansion of the liquid phase and as being able to distinguish between the volume expansion behavior of all combinations of antisolvent–solvent

$$\frac{\Delta V}{V} = \frac{v_{mix}(T, p, x_{CO_2}) - v_{IL}(T, p_0)}{v_{IL}(T, p_0)} \tag{15}$$

where v_{mix} is the mixture molar volume at a given temperature, pressure and carbon dioxide molar fraction and v_{IL} is the IL molar volume at the same temperature and at 0.1 MPa.

Although the result of the relative expansions introduce more definition on the volume expansions analysis, the results still indicate a strong dependence on the solvent family and most important on the type of gas sorption mechanism.

As depicted in Fig. 7, upon the CO_2 addition the molar volume decreases for all the compound families. The only exception

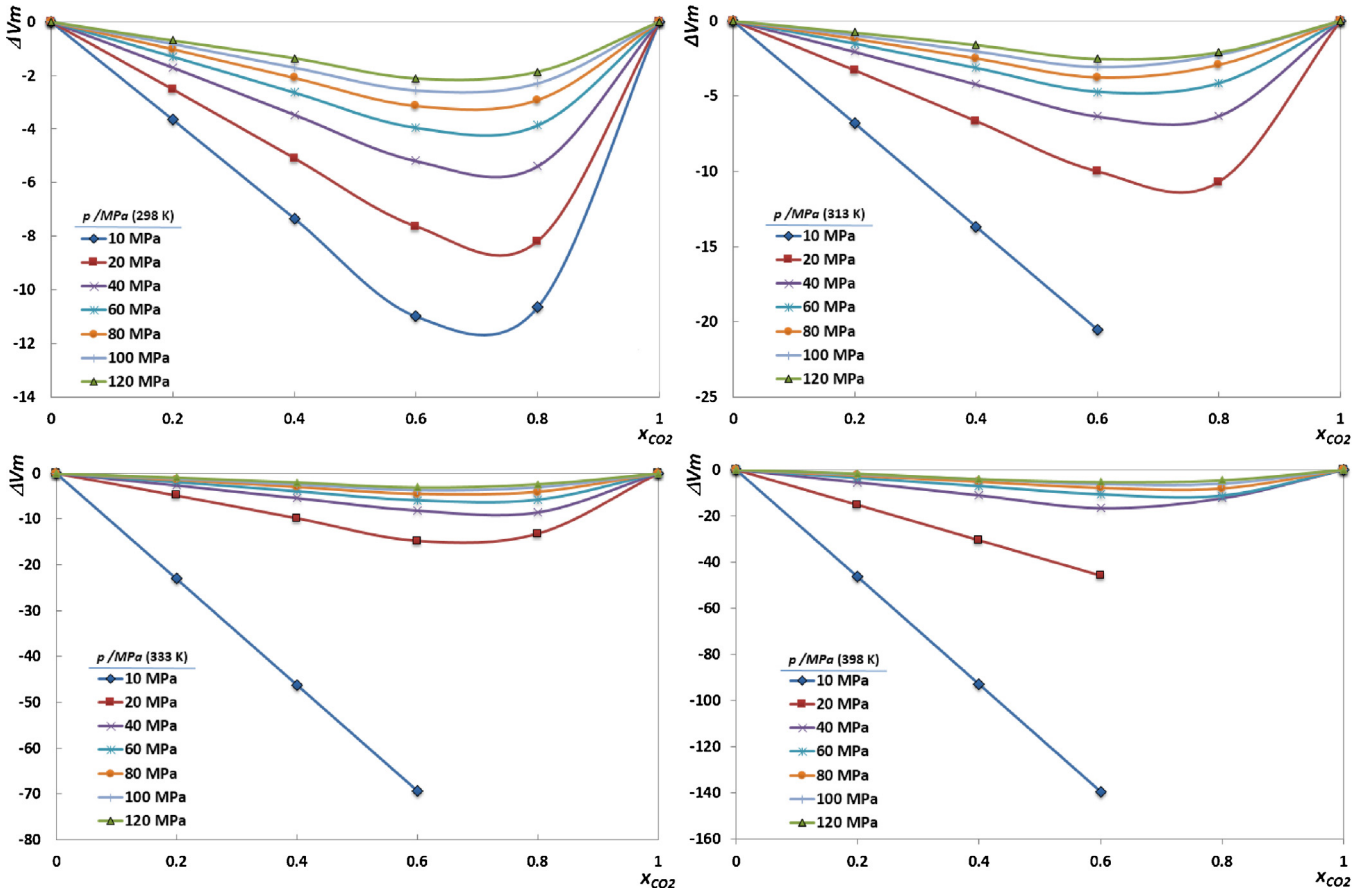

Fig. 5. Excess molar volume as function of CO_2 mole fractions, for the system CO_2 + [C_2mim][$EtSO_4$], at 298 K (top left), 313 K (top right), 333 K (bottom left) and 398 K (bottom right).

is found for the acetonitrile that, even though the molar volume decreases initially, starts to increase for CO_2 mole fractions higher than 0.6, ending to present positive relative expansions for CO_2 mole fractions higher than 0.88. Alkanes present slightly lower relative expansions than the selected IL, however, this behavior seems to be related to the IL high polarity and consequently to its lower solubility, compared to other non-task-specific ILs.

Both approaches, volume expansion, relative volume expansion and excess molar volume, point out to a dissolution mechanism for the carbon dioxide in alkanes and ILs where the gas upon dissolution occupies only the bulk free volume, leading thus to an increase on the mixture density, and that these compounds do not expand significantly upon gas addition. Thus, one may envision both ILs and alkanes as a porous media or sponge-like pseudo-rigid structure with large amounts of free volume in which the carbon dioxide is able to accommodate without significantly interacting with the solvent, in good agreement with the mechanism derived from Raman spectra by Cabaço et al. [15].

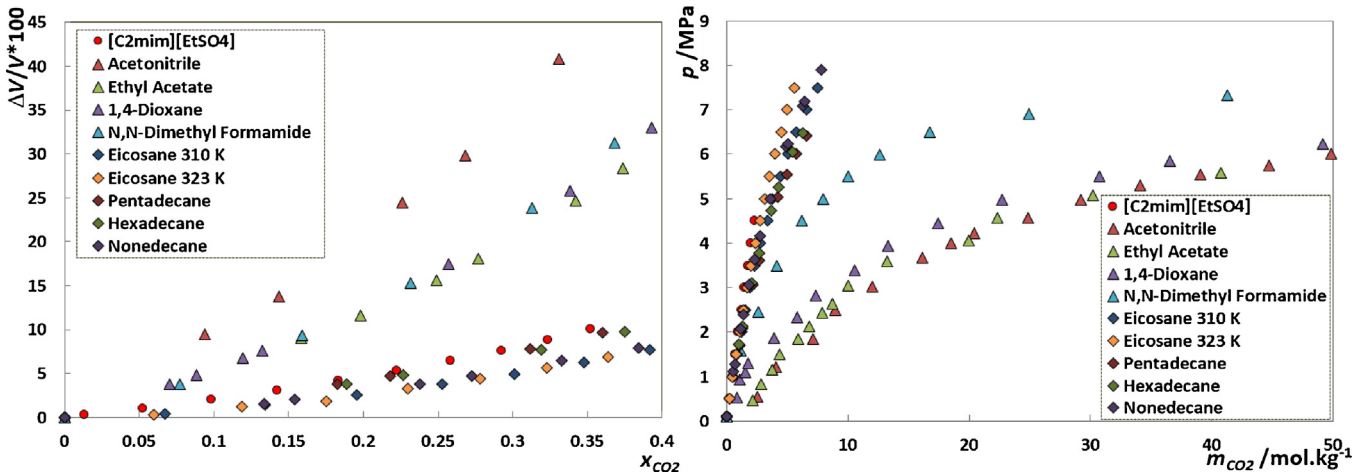

Fig. 6. Volume expansion of the liquid phase of a CO_2-expanded organic solvent (left), determined using Eq. (14), and pressure–molality phase diagram (right) of several binary systems at 313 K [40–45].

Table 5
Experimental density (ρ) data as function of temperature, pressure and CO_2 composition.

T (K)	278.15	298.15	313.15	333.15	348.15	373.15	398.15	278.15	298.15	313.15	333.15	348.15	373.15	398.15	278.15	298.15	313.15	333.15	348.15	373.15	398.15
p (MPa)	$x_{CO_2} = 0$[a]							$x_{CO_2} = 0.2007$							$x_{CO_2} = 1$[b]						
0.1	1.2528	1.2375	1.2270	1.2132	1.2033	1.1874	1.1715								0.001915	0.001784	0.001697	0.001594	0.001525	0.001422	0.001332
1	1.2532	1.2379	1.2274	1.2136	1.2038	1.1874	1.1711								0.020367	0.018716	0.017669	0.016464	0.015673	0.014525	0.013544
10	1.2567	1.2415	1.2312	1.2176	1.2079	1.1920	1.1760	1.2550	1.2413	1.2306	1.2170	1.2072	1.1908	1.1752	0.9483	0.8176	0.6286	0.2900	0.2334	0.1886	0.1630
20	1.2605	1.2456	1.2354	1.2220	1.2125	1.1968	1.1811	1.2587	1.2452	1.2347	1.2213	1.2117	1.1956	1.1803	1.0007	0.9142	0.8398	0.7237	0.6262	0.4805	0.3858
40	1.2677	1.2532	1.2433	1.2303	1.2211	1.2059	1.1908	1.2661	1.2529	1.2426	1.2296	1.2202	1.2047	1.1899	1.0663	1.0042	0.9561	0.8901	0.8399	0.7567	0.6776
60	1.2746	1.2604	1.2508	1.2382	1.2292	1.2144	1.1998	1.2730	1.2602	1.2502	1.2374	1.2283	1.2132	1.1989	1.1113	1.0593	1.0201	0.9677	0.9287	0.8649	0.8037
80	1.2812	1.2673	1.2578	1.2455	1.2367	1.2224	1.2082	1.2795	1.2670	1.2573	1.2448	1.2359	1.2212	1.2072	1.1464	1.1003	1.0659	1.0206	0.9871	0.9327	0.8806
100	1.2875	1.2740	1.2647	1.2526	1.2440	1.2299	1.2161	1.2858	1.2737	1.2640	1.2518	1.2432	1.2287	1.2152	1.1754	1.1333	1.1022	1.0614	1.0314	0.9828	0.9362
120	1.2932	1.2802	1.2712	1.2595	1.2511	1.2372	1.2236	1.2917	1.2801	1.2706	1.2586	1.2501	1.2361	1.2227	1.2003	1.1612	1.1324	1.0949	1.0673	1.0228	0.9800
p (MPa)	$x_{CO_2} = 0.6009$							$x_{CO_2} = 0.7987$							$x_{CO_2} = 0.4007$						
10	1.2549	1.2410	1.2306	1.2169	1.2071	1.1906	1.1743	1.2188	1.1700							1.2552	1.2413	1.2308	1.2173	1.2074	1.1909	1.1750
20	1.2588	1.2451	1.2348	1.2213	1.2117	1.1954	1.1796	1.2262	1.2081	1.1871	1.1134					1.2591	1.2453	1.2349	1.2216	1.2119	1.1957	1.1801
40	1.2661	1.2527	1.2427	1.2297	1.2203	1.2046	1.1894	1.2345	1.2238	1.2035	1.1882	1.1729	1.1285	1.0407		1.2665	1.2530	1.2428	1.2299	1.2205	1.2048	1.1898
60	1.2731	1.2601	1.2503	1.2376	1.2285	1.2132	1.1985	1.2435	1.2333	1.2102	1.1992	1.1895	1.1700	1.1472		1.2735	1.2603	1.2503	1.2377	1.2286	1.2133	1.1988
80	1.2797	1.2670	1.2575	1.2451	1.2361	1.2213	1.2070	1.2539	1.2425	1.2183	1.2077	1.1981	1.1819	1.1652		1.2801	1.2671	1.2574	1.2451	1.2362	1.2214	1.2071
100	1.2861	1.2737	1.2643	1.2522	1.2435	1.2290	1.2151	1.2659	1.2520	1.2295	1.2166	1.2067	1.1896	1.1739		1.2865	1.2738	1.2643	1.2521	1.2435	1.2290	1.2152
120	1.2922	1.2802	1.2708	1.2588	1.2504	1.2362	1.2225	1.2793	1.2616	1.2458	1.2256	1.2173	1.1948	1.1783		1.2917	1.2796	1.2701	1.2583	1.2503	1.2382	1.2280

[a] Data taken from previous work [19].
[b] Data taken from NIST [37].

Fig. 7. Relative volume expansion of the liquid phase of a CO_2-expanded organic solvent, determined using Eq. (15), at 313 K.

4. Conclusions

The CO_2 solubility in $[C_2mim][EtSO_4]$ was investigated in the temperature range 273–413 K, for pressures up to 5 MPa and CO_2 mole fractions ranging from 0.02 to 0.5, using the isochoric method. The IL presents positive deviations from ideality and similar to what was observed previously for phosphonate-based ILs, the highly polar sulfate IL presents unfavorable interactions toward the CO_2. The results emphasize that if one targets a highly selective solvent for carbon dioxide separation a delicate balance between the solvent polarity and the molar volume must be established.

Density measurements for the CO_2 + $[C_2mim][EtSO_4]$ system were carried out at temperatures ranging from 278.15 K to 398.15 K, pressures from 10 MPa to 120 MPa and for 0.2, 0.4, 0.7 and 0.8 CO_2 mole fractions. The results show that the pressure has no significant influence on the density, for carbon dioxide mole fractions up to 0.6. For higher CO_2 mole fractions, nonetheless, the densities are greatly affected by pressure. The system studied presents negative excess molar volumes over the whole range of compositions and temperatures. The observed system contraction results from the large difference between the molecular volumes of the species involved, with the small carbon dioxide molecules occupying the empty spaces between the larger volumes of the IL ions. The volume expansion of this system supports the idea that the carbon dioxide, upon dissolution, occupies only the bulk free volume since the IL does not expand upon the gas addition. These findings are also supported by the negative values of the entropy of solvation that indicate an increase in order of the solvent molecules surrounding the solute.

The result suggest that both IL and alkane systems may be envisioned as a porous media or a sponge-like pseudo-rigid structure with large amounts of free volume in which the carbon dioxide is able to accommodate itself with little interaction with the solvent.

Acknowledgements

The authors acknowledge the financial support from FCT–Fundação para a Ciência e a Tecnologia through the projects PTDC/QUI-QUI/121520/2010 and Pest-C/CTM/LA0011/2013 and post-doctoral Grant SFRH/BPD/82264/2011 of P.J.C. J.F. and T.R. are grateful to Ministry of Science and Innovation (Spain) by the support through the project CTQ2011-23925. L.L. acknowledges to this Ministry the financial support of Ramon y Cajal Program. We are also grateful to Xunta de Galicia for the financial support of the Galician Network on ILs, ReGaLIs (CN2012/210).

References

[1] A. Yokozeki, D.J. Kasprzak, M.B. Shiflett, Thermal effect on C—H stretching vibrations of the imidazolium ring in ionic liquids, Physical Chemistry Chemical Physics 9 (2007) 5018–5026.

[2] N.M.B. Flichy, S.G. Kazarian, C.J. Lawrence, B.J. Briscoe, An ATR-IR study of poly(dimethylsiloxane) under high-pressure carbon dioxide: simultaneous measurement of sorption and swelling, J. Physical Chemistry B 106 (2002) 754–759.

[3] L. Cammarata, S.G. Kazarian, P.A. Salter, T. Welton, Molecular states of water in room temperature ionic liquids, Physical Chemistry Chemical Physics 3 (2001) 5192–5200.

[4] L. Crowhurst, P.R. Mawdsley, J.M. Perez-Arlandis, P.A. Salter, T. Welton, Solvent–solute interactions in ionic liquids, Physical Chemistry Chemical Physics 5 (2003) 2790.

[5] J. Andanson, F. Jutz, A. Baiker, Supercritical CO_2/ionic liquid systems: what can we extract from infrared and Raman spectra? J. Physical Chemistry B 113 (2009) 10249–10254.

[6] B.L. Bhargava, S. Balasubramanian, Probing anion–carbon dioxide interactions in room temperature ionic liquids: gas phase cluster calculations, Chemical Physics Letters 444 (2007) 242–246.

[7] B.L. Bhargava, S. Balasubramanian, Insights into the structure and dynamics of a room-temperature ionic liquid: ab initio molecular dynamics simulation studies of 1-n-butyl-3-methylimidazolium hexafluorophosphate ([bmim][PF6]) and the [bmim][PF6]-CO_2 mixture, J. Physical Chemistry B 111 (2007) 4477–4487.

[8] T. Seki, J.-D. Grunwaldt, A. Baiker, In situ attenuated total reflection infrared spectroscopy of imidazolium-based room-temperature ionic liquids under supercritical CO_2, J. Physical Chemistry B 113 (2009) 114–122.

[9] P.J. Carvalho, J.A.P. Coutinho, On the nonideality of CO_2 solutions in ionic liquids and other low volatile solvents, J. Physical Chemistry Letters 1 (2010) 774–780.

[10] P.J. Carvalho, J.A.P. Coutinho, The polarity effect upon the methane solubility in ionic liquids: a contribution for the design of ionic liquids for enhanced CO_2/CH_4 and H_2S/CH_4 selectivities, Energy Environmental Science 4 (2011) 4614.

[11] L.M.C. Pereira, M.B. Oliveira, A.M.A. Dias, F. Llovell, L.F. Vega, P.J. Carvalho, et al., High pressure separation of greenhouse gases from air with 1-ethyl-3-methylimidazolium methyl-phosphonate, International Journal of Greenhouse Gas Control 19 (2013) 299–309.

[12] S.G. Kazarian, B.J. Briscoe, T. Welton, Combining ionic liquids and supercritical fluids: in situ ATR-IR study of CO_2 dissolved in two ionic liquids at high pressures, Chemical Communications (2000) 2047–2048.

[13] W. Shi, E.J. Maginn, Atomistic simulation of the absorption of carbon dioxide and water in the ionic liquid 1-n-hexyl-3-methylimidazolium bis(trifluoromethylsulfonyl)imide ([hmim][Tf2N]), J. Physical Chemistry B 112 (2008) 2045–2055.

[14] X. Huang, C.J. Margulis, Y. Li, B.J. Berne, Why is the partial molar volume of CO_2 so small when dissolved in a room temperature ionic liquid? Structure and dynamics of CO_2 dissolved in [Bmim+] [PF6−], J. American Chemical Society 127 (2005) 17842–17851.

[15] M.I. Cabaço, M. Besnard, Y. Danten, J.A.P. Coutinho, Solubility of CO_2 in 1-butyl-3-methyl-imidazolium-trifluoro acetate ionic liquid studied by Raman spectroscopy and DFT investigations, J. Physical Chemistry B 115 (2011) 3538–3550.

[16] S.N.V.K. Aki, B.R. Mellein, E.M. Saurer, J.F. Brennecke, High-pressure phase behavior of carbon dioxide with imidazolium-based ionic liquids, J. Physical Chemistry B 108 (2004) 20355–20365.

[17] D. Kodama, M. Kanakubo, M. Kokubo, T. Ono, H. Kawanami, T. Yokoyama, et al., CO_2 absorption properties of Brønsted acid–base ionic liquid composed of N,N-dimethylformamide and bis(trifluoromethanesulfonyl)amide, J. Supercritical Fluids 52 (2010) 189–192.

[18] J. Safarov, R. Hamidova, M. Stephan, N. Schmotz, I. Kul, A. Shahverdiyev, et al., Carbon dioxide solubility in 1-butyl-3-methylimidazolium-bis(trifluormethylsulfonyl)imide over a wide range of temperatures and pressures, J. Chemical Thermodynamics 67 (2013) 181–189.

[19] T. Regueira, L. Lugo, J. Fernández, High pressure volumetric properties of 1-ethyl-3-methylimidazolium ethylsulfate and 1-(2-methoxyethyl)-1-methyl-pyrrolidinium bis(trifluoromethylsulfonyl)imide, J. Chemical Thermodynamics 48 (2012) 213–220.

[20] O. Fandiño, L. Lugo, J.J. Segovia, E.R. López, M.J.P. Comuñas, J. Fernández, High pressure densities of carbon dioxide + dipentaerythritol hexaheptanoate: new experimental setup and volumetric behavior, J. Supercritical Fluids 58 (2011) 189–197.

[21] B. Lagourette, C. Boned, H. Saint-Guirons, P. Xans, H. Zhou, Densimeter calibration method versus temperature and pressure, Measurement Science and Technology 3 (1992) 699.

[22] M.J.P. Comuñas, J. Bazile, A. Baylaucq, C. Boned, Density of diethyl adipate using a new vibrating tube densimeter from (293.15 to 403.15) K and up to 140 MPa calibration and measurements, J. Chemical Engineering Data 53 (2008) 986–994.

[23] J.J. Segovia, O. Fandiño, E.R. López, L. Lugo, M.C. Martín, J. Fernández, Automated densimetric system: measurements and uncertainties for compressed fluids, J. Chemical Thermodynamics 41 (2009) 632–638.

[24] P.J. Carvalho, V.H. Álvarez, J.J.B. Machado, J. Pauly, J.-L. Daridon, I.M. Marrucho, et al., High pressure phase behavior of carbon dioxide in 1-alkyl-3-methylimidazolium bis(trifluoromethylsulfonyl)imide ionic liquids, J. Supercritical Fluids 48 (2009) 99–107.

[25] P.J. Carvalho, V.H. Alvarez, B. Schröder, A.M. Gil, I.M. Marrucho, M. Aznar, et al., Specific solvation interactions of CO_2 on acetate and trifluoroacetate imidazolium based ionic liquids at high pressures, J. Physical Chemistry B 113 (2009) 6803–6812.

[26] P.J. Carvalho, V.H. Álvarez, I.M. Marrucho, M. Aznar, J.A.P. Coutinho, High pressure phase behavior of carbon dioxide in 1-butyl-3-methylimidazolium bis(trifluoromethylsulfonyl)imide and 1-butyl-3-methylimidazolium dicyanamide ionic liquids, J. Supercritical Fluids 50 (2009) 105–111.

[27] S. Mattedi, P.J. Carvalho, J.A.P. Coutinho, V.H. Alvarez, M. Iglesias, High pressure CO_2 solubility in N-methyl-2-hydroxyethylammonium protic ionic liquids, J. Supercritical Fluids 56 (2011) 224–230.

[28] L.A. Blanchard, Z. Gu, J.F. Brennecke, High-pressure phase behavior of ionic liquid/CO_2 systems, J. Physical Chemistry B 105 (2001) 2437–2444.

[29] A.H. Jalili, A. Mehdizadeh, M. Shokouhi, A.N. Ahmadi, M. Hosseini-Jenab, F. Fateminassab, Solubility and diffusion of CO_2 and H_2S in the ionic liquid 1-ethyl-3-methylimidazolium ethylsulfate, J. Chemical Thermodynamics 42 (2010) 1298–1303.

[30] M.D. Bermejo, T.M. Fieback, Á. Martín, Solubility of gases in 1-alkyl-3methylimidazolium alkyl sulfate ionic liquids: experimental determination and modeling, J. Chemical Thermodynamics 58 (2013) 237–244.

[31] A.N. Soriano, B.T. Doma Jr., M.-H. Li, Carbon dioxide solubility in some ionic liquids at moderate pressures, J. Taiwan Institute of Chemical Engineers 40 (2009) 387–393.

[32] S. Supasitmongkol, P. Styring, High CO_2 solubility in ionic liquids and a tetraalkylammonium-based poly(ionic liquid), Energy Environmental Science 3 (2010) 1961.

[33] M. Petermann, T. Weissert, S. Kareth, H.W. Lösch, F. Dreisbach, New instrument to measure the selective sorption of gas mixtures under high pressures, J. Supercritical Fluids 45 (2008) 156–160.

[34] M.D. Bermejo, M. Montero, E. Saez, L.J. Florusse, A.J. Kotlewska, M.J. Cocero, et al., Liquid–vapor equilibrium of the systems butylmethylimidazolium nitrate-CO_2 and hydroxypropylmethylimidazolium nitrate-CO_2 at high pressure: influence of water on the phase behavior, J. Physical Chemistry B 112 (2008) 13532–13541.

[35] J. Jacquemin, P. Goodrich, W. Jiang, D.W. Rooney, C. Hardacre, Are alkyl sulfate-based protic and aprotic ionic liquids stable with water and alcohols? A thermodynamic approach, J. Physical Chemistry B 117 (2013) 1938–1949.

[36] R. Span, W. Wagner, A new equation of state for carbon dioxide covering the fluid region from the triple-point temperature to 1100 K at pressures up to 800 MPa, J. Physical and Chemical Reference Data 25 (1996) 1509.

[37] P.J. Linstrom, W.G. Mallard (Eds.), NIST Chemistry WebBook, NIST Standard Reference Database Number 69, Natl. Inst. Stand. Technol., Gaithersbg, MD, 2013 http://www.webbook.nist.gov

[38] A.S. Pensado, A.A.H. Pádua, M.J.P. Comuñas, J. Fernández, High-pressure viscosity and density of carbon dioxide + pentaerythritol ester mixtures: measurements and modeling, AIChE J. 54 (2008) 1625–1636.

[39] A.S. Pensado, A.A.H. Pádua, M.J.P. Comuñas, J. Fernández, Viscosity and density measurements for carbon dioxide + pentaerythritol ester lubricant mixtures at low lubricant concentration, J. Supercritical Fluids 44 (2008) 172–185.

[40] A. Kordikowski, A.P. Schenk, R.M. Van Nielen, C.J. Peters, Volume expansions and vapor–liquid equilibria of binary mixtures of a variety of polar solvents and certain near-critical solvents, J. Supercritical Fluids 8 (1995) 205–216.

[41] N. Nagarajan, R.L. Robinson, Equilibrium phase compositions, phase densities, and interfacial tensions for carbon dioxide + hydrocarbon systems. 2. Carbon dioxide + n-decane, J. Chemical Engineering Data 31 (1986) 168–171.

[42] N.C. Huie, K.D. Luks, J.P. Kohn, Phase-equilibriums behavior of systems carbon dioxide-n-eicosane and carbon dioxide-n-decane-n-eicosane, J. Chemical Engineering Data 18 (1973) 311–313.

[43] D.J. Fall, K.D. Luks, Liquid–liquid–vapor phase equilibria of the binary system carbon dioxide + n-tridecane, J. Chemical Engineering Data 30 (1985) 276–279.

[44] H. Tanaka, Y. Yamaki, M. Kato, Solubility of carbon dioxide in pentadecane, hexadecane, and pentadecane + hexadecane, J. Chemical Engineering Data 38 (1993) 386–388.

[45] L. Cited, D.J. Fall, J.L. Fail, D. Kraemer, J.L. Fall, K.D. Luks, Liquid–liquid–vapor immiscibility limits in carbon dioxide + *n*-paraffin mixtures, J. Chemical Engineering Data 30 (1985) 82–88.

[46] J.C. de la Fuente Badilla, C.J. Peters, J. de Swaan Arons, Volume expansion in relation to the gas–antisolvent process, J. Supercritical Fluids 17 (2000) 13–23.

[47] C.-S. Su, Prediction of volumetric properties of carbon dioxide-expanded organic solvents using the predictive Soave–Redlich–Kwong (PSRK) equation of state, J. Supercritical Fluids 72 (2012) 223–231.

[48] P.J. Carvalho, J.A.P. Coutinho, Non-ideality of solutions of NH_3, SO_2, and H_2S in ionic liquids and the prediction of their solubilities using the Flory–Huggins model, Energy & Fuels 24 (2010) 6662–6666.